



# Macro X-ray fluorescence scanning (MA-XRF) as tool in the authentication of paintings



Steven Saverwyns<sup>a,\*</sup>, Christina Currie<sup>b</sup>, Eduardo Lamas-Delgado<sup>c</sup>

<sup>a</sup> Royal Institute for Cultural Heritage (KIK-IRPA), Laboratories Department, Painting Laboratory, Jubelpark 1, 1000 Brussels, Belgium

<sup>b</sup> Royal Institute for Cultural Heritage (KIK-IRPA), Documentation Department, Scientific Imagery, Jubelpark 1, 1000 Brussels, Belgium

<sup>c</sup> Royal Institute for Cultural Heritage (KIK-IRPA), Documentation Department, Library and Inventory, Belgium

## ARTICLE INFO

### Article history:

Received 24 July 2017

Received in revised form 3 October 2017

Accepted 12 October 2017

Available online 16 October 2017

### Keywords:

Authenticity

Paintings

Macro X-ray fluorescence (MA-XRF)

Scientific imaging

## ABSTRACT

Scanning macro X-ray fluorescence (MA-XRF) was evaluated as a means for the non-invasive study of two paintings to investigate their authenticity. The first painting, a still-life attributed to the 17th century Spanish painter Francisco de Zurbarán, was analysed both with point XRF analyses and MA-XRF. MA-XRF analyses facilitated the interpretation of the results, revealed a hidden painting and gave a clear answer on the question of authenticity. The second painting, attributed to the workshop or school of Pieter Paul Rubens, was investigated by MA-XRF alone. This revealed a hidden stamp of a canvas manufactory, which situated the painting a few hundred years later than originally supposed. In this last case MA-XRF results were supported by X-radiography and infrared reflectography (IRR). A brief comparison was made between MA-XRF and these traditional scientific imaging techniques, which were not able to detect the stamp. Moreover, it is suggested that in certain cases where for budgetary reasons X-radiographs cannot be made, MA-XRF images can sometimes suffice.

© 2017 Elsevier B.V. All rights reserved.

## 1. Introduction

Copies and forgeries have been around since the art market came into existence. The idea of making money - the main reason for the production of falsifications - by producing art in the style of a well-known artist has always been attractive to criminal minds. Although art works of all kinds have been falsified or copied [1–3], the emphasis in this paper is on paintings. Over the last decades the buying of art as a long-term investment has boomed, and the art market is therefore increasingly attractive to fraudsters. It has witnessed many scandals [4, 5], and although cases of fraud have been known since the Renaissance - even Michelangelo supposedly forged a classical sculpture by artificially aging it [3] - the most notorious cases date from after the Second World War. One of the most famous is the Van Meegeren affair, when Dutch artist Han van Meegeren falsified old Master paintings, including paintings by Johannes Vermeer [6,7]. One of these paintings ended up in the collection of *Reichsmarschall* Hermann Göring during the Nazi occupation of the Netherlands. After the Second World War, Van Meegeren was accused of collaboration for having sold Dutch art to the enemy and in order to avoid a death sentence, he confessed that the painting was in fact a fake. During the trial, a team of scientists led by Paul Coremans, the later founder of the Royal Institute for Cultural Heritage, proved by chemical analysis that the painting contained 20th century

paint hardeners, hence ruling out the attribution to Vermeer [8]. This is also one of the first cases where exact science could prove a painting to be a later copy. In the following decades the art market was disrupted by forgeries on a large scale. Well-known cases include forgeries by Elmyr de Hory [9], John Myatt [10], Wolfgang Beltracchi [11–13] and Pei-Shen Qian [14]. Besides these great scandals, many other lesser-known forgeries have come onto the market [15–18]. These can lead to a crisis of confidence in the art market, as the value of a painting largely depends on its attribution to a known artist. For art historians forgeries are also problematic, as they falsify history, especially when they are not (yet) exposed as being fake.

In authenticity matters, the opinion of the expert or connoisseur has long been the only source on which the final verdict is based [19]. Comparison of the style and technique of the painting under investigation with that of known and well-established paintings by the master to whom the painting is attributed lead to a judgement on authenticity. Provenance studies, in which the history of the painting is traced back to the artist himself, can sometimes support the opinion of the expert. Since the 20th century, and especially since the second half of the 20th century, exact science has played an increasingly important role in these kinds of studies. Although analyses alone cannot prove the authenticity of a painting, it can sometimes disprove an early dating or strengthen the case for authenticity. In the aforementioned Beltracchi case, it was the finding of one anachronistic pigment - titanium white - in a falsified painting that triggered further research and exposed the scandal [13,20]. This does not imply that the eye of the expert is less

\* Corresponding author.

E-mail address: [steven.saverwyns@kikirpa.be](mailto:steven.saverwyns@kikirpa.be) (S. Saverwyns).

important than before. Indeed, it is only through the synergy of connoisseurship, provenance studies and exact science that real progress can be made in the battle against forgeries.

The arsenal of analytical techniques is ever expanding as science develops. Well-established techniques include scientific imagery methods like X-radiography [21] and infrared reflectography [22], which reveal underlayers and underdrawings respectively and give important art historical and technological information on the works examined [1]. However, scientific analysis of materials paintings are made of is playing an increasingly key role in the investigation of possible forgeries, especially in the identification of anachronistic materials. Both a painting's support and its painting materials can be analysed. In terms of the support, dating methods are often of crucial importance, namely  $^{14}\text{C}$ -dating and dendrochronology [1]. Painting materials are investigated by a large range of scientific methods such as scanning electron microscopy (SEM), X-ray fluorescence (XRF), micro-Raman spectroscopy (MRS), pyrolysis gas chromatography mass spectrometry (Py-GCMS) and high-performance liquid chromatography (HPLC) to name only the most commonly used ones [23]. The development of new analytical techniques and applications has helped advance the fight against counterfeiting. Although micro-Raman spectroscopy has been used for the identification of pigments in artworks since the late 1990s, the potential of the technique for the identification of synthetic organic pigments was only fully exploited a decade later [24–27] and has since played an important role in the characterisation of the palettes of modern and contemporary artists [28,29] and in the exposure of many artworks as fakes [16–18,30].

XRF has long been an established technique for the study of painting materials owing to its non-invasiveness, speed of analysis, good spatial resolution and the fact that information from both the surface and underlayers can be obtained in one measurement. However, some of these features are also drawbacks. Pigments (or other inorganic materials) in different layers all produce secondary X-rays, complicating the interpretation of results. Furthermore, due to the limited number of spots that can be analysed in a feasible amount of time, only local point information is obtained, which is not necessarily representative of the whole painting. The recent introduction of macro X-ray fluorescence (MA-XRF) deals effectively with some of these drawbacks [31–35]. In MA-XRF the X-ray beam scans areas or even the whole painting, producing thousands and sometimes millions of data points. Results can be plotted as elemental distribution maps. These images can make interpretation more straightforward and since the points analysed cover a wide surface area, they are more representative of the whole painting. Moreover, discussing images instead of raw spectra with conservators, art-historians and other non-XRF experts is infinitely more conducive to useful exchanges during multidisciplinary projects.

This paper discusses the benefits of MA-XRF for the authentication of paintings [32,36,37] in comparison with classic point XRF measurements and scientific imagery (mainly X-radiography). Two case studies

are presented, a still-life painting attributed to the Spanish painter Francisco de Zurbarán and a Portrait of Jan Brant, attributed to the workshop or school of Rubens.

## 2. Experimental

### 2.1. Paintings under investigation

#### 2.1.1. Still-life painting attributed to Francisco de Zurbarán (1598–1664), private collection

The work investigated (Fig. 1a) is a still-life painted in oil on canvas ( $104.5 \times 146.5$  cm). Stylistically, it recalls Spanish painting from the second third of the 17th century. The painting arrived at the Royal Institute for Cultural Heritage with an attribution to the Sevillian painter Francisco de Zurbarán (1598–1664). A thorough stylistic study showed that certain elements are indeed similar to still-lives carried out by Zurbarán, but the style of the composition is more characteristic of Sevillian and Madrilénian still-lives from the 1630s. The neutral dark background and the arrangement of the objects on a stone shelf are characteristic of Spanish still-lives of this period, especially those originating from Madrid. The arrangement of the fruit on a metal tray, probably pewter or silver, is often seen in other still-lives by Zurbarán, but also features in many Spanish still-lives of the period, especially from Madrid, as in the work of Juan Van der Hamen y León (1596–1631) and Antonio Ponce (1608–1677).

The painting does include motifs, however, that do not fit with the period in question. The typology of the metal jug on the left, for example, does not correspond to that of contemporary Spanish silverware. Its decoration is atypical for the Baroque period, suggesting instead a 19th century origin. It could be an element added at a later date. Moreover, the lobster at the foot of the jug also raises doubts, as to the best of our knowledge no other Spanish still-life paintings of the period are known to depict lobsters. Finally, the vase with lilies is not painted with the finesse of brushwork seen in the flowers and plate with grapes, suggesting possible repainting.

On the basis of artistic style, it was concluded that the painting might have originated in 17th century Spain, possibly modified in the 19th or 20th century by the addition of elements such as the lobster, metal jug and vase with flowers. The style of the older motifs situates the painting in the context of still-life painters of the school of Madrid active in the middle of the 17th century, such as Antonio Ponce and Francisco Barrera. Attribution to Francisco de Zurbarán seems unlikely.

#### 2.1.2. Portrait of Jan Brant attributed to the workshop or school of Pieter Paul Rubens (1577–1640), private collection

The second painting (Fig. 2a) studied with MA-XRF is also painted in oil on canvas ( $65.5 \times 56.5$  cm). It is a faithful copy of Rubens's Portrait of Jan Brant in the Alte Pinakothek in Munich [38]. Jan Brant was Rubens's father-in-law as well as an important Antwerp humanist, lawyer,



Fig. 1. Still-life painting, formerly attributed to Francisco de Zurbarán (1598–1664), oil on canvas ( $104.5 \times 146.5$  cm), private collection, under a) normal light and b) UV-light illumination.



**Fig. 2.** Portrait of Jan Brant, formerly attributed to workshop or school of Pieter Paul Rubens (1577–1640), oil on canvas (65.5 × 56.5 cm), private collection, under a) normal light and b) UV-light illumination.

alderman and town clerk. The painting was studied at the request of the Rubenshuis in Antwerp to learn more about its techniques and materials. The aim of the investigation was to find out whether the painting could be a contemporary copy, perhaps painted in Rubens's workshop, or a later copy.

The painting, smaller in size than the original version, only depicts parts of the original composition: the artists focused on the head, torso and ruff, rather than the larger composition with bookshelf, hands and book. During the study, X-radiography and infrared reflectography were also carried out, making it possible to compare the chemical imaging features of MA-XRF with these more traditional types of imaging.

## 2.2. Materials and methods

### 2.2.1. XRF instrumentation

XRF spectra were obtained with an ARTAX micro-XRF instrument (Bruker AXS, Germany) [39] equipped with a rhodium tube as X-ray source and a thermo-electrically cooled Si-drift detector. A poly-capillary lens was used to reduce the X-ray beam diameter to ca. 70  $\mu\text{m}$  with high fluorescence intensity, while a CCD camera allowed the positioning of the X-ray beam on the object. All measurements were performed under the following experimental conditions: accelerating voltage of 50 kV, current of 600  $\mu\text{A}$  and measurement time of 60 s.

### 2.2.2. MA-XRF instrumentation

MA-XRF maps were registered using the M6 Jetstream large area scanner (Bruker AXS, Berlin, Germany) [32]. The heart of the instrument consists of a Rh-target microfocus X-ray tube operated at 50 kV and 600  $\mu\text{A}$  current, and a 30  $\text{mm}^2$  X-Flash silicon drift detector (energy resolution < 145 eV at Mn-K $\alpha$ ). The X-ray beam size is defined by poly-capillary optics and is determined by the distance between the measuring head and the painting. In order to allow scanning, the measuring head is mounted on an XY-motorized stage with maximum travelling range of 80 × 60 cm in steps as small as 10  $\mu\text{m}$ . Both paintings were scanned using an X-ray beam size of 500  $\mu\text{m}$ , in steps of 500  $\mu\text{m}$ , and a dwell time per step of 10 ms. The spectra were collected, deconvoluted and examined with the Bruker M6 Jetstream software. Chemical elements were identified in the scan by examining the sum spectrum and maximum pixel spectra [40].

### 2.2.3. Micro-Raman spectroscopy

As XRF is an elemental technique, only capable of detecting inorganic compounds, additional Raman measurements were carried out in a limited number of areas to clarify or refine some of the analysis results obtained by XRF. Raman spectra were acquired with a Renishaw inVia Raman microscope (Wotton-under-Edge, UK) with a Peltier-cooled (203 K), near-infrared enhanced, deep-depletion CCD detector (576 × 384 pixels) using a high power 785 nm diode laser (Innovative Photonic Solutions, New Jersey, USA) in combination with a 1200 l/mm grating. Laser power was reduced to ca. 0.5 mW with neutral density filters. Analyses were performed directly on the painting with a fibre-coupled Raman probe for 785 nm excitation as described in detail elsewhere [41]. Identification of the Raman spectrum was done by comparison with in-house compiled reference spectra.

### 2.2.4. X-radiography set-up

The “Portrait of Jan Brant” was radiographed using a Baltograph generator (Balteau NDT, Hermalle-sous-Argenteau, Belgium) operated at 50 kV with a current of 15 mA. The distance between the instrument and the painting was 6 m, and an exposition time of 240 s was applied. The X-radiograph was recorded on two Agfa Structurix D4 films. The films were scanned and the digital images stitched together using Photoshop to produce the final image.

### 2.2.5. IRR set-up

Infrared reflectograms of the “Portrait of Jan Brant” were taken using a Lion systems (Luxembourg, Luxembourg) thermal camera sensitive to near infrared radiation in the 900–1700 nm spectral range. The image is captured using a 50 mm Nikkor lens (Nikon) in combination with a 1500–1730 nm filter, and registered with an InGaAs sensor with a resolution of 512 × 640 pixels. The entire surface of the painting is recorded as a series of small images. A motorized rail system is used for precise positioning of the camera. The platform moves vertically, horizontally and diagonally and has a laser-guided forwards/backwards feature to maintain a constant distance between the camera and the painting. Warps or irregularities in the painting's surface are thus accommodated, ensuring that images are focused and remain the same size. Capturing images is carried out manually, by remote control, using Wi-Fi and dedicated software. The recorded images are digitised and assembled using



Adobe Photoshop or PTGui, resulting in high quality, seamless infrared reflectograms.

### 3. Results and discussion

The still-life painting was examined first with point XRF spectroscopy. As questions remained unanswered, the painting was reinvestigated in a second phase after the acquisition of the MA-XRF instrument. The Portrait of Jan Brant was only investigated by MA-XRF, but additional classic scientific imagery was performed.

#### 3.1. XRF vs. MA-XRF on the still-life painting

Following usual practice, the painting was first examined with ultraviolet light to attempt to localise later overpaint or retouching (Fig. 1b). This excited a bluish fluorescence in the thick varnish layer; in some places drips are clearly visible. The strong fluorescence, however, completely masked possible later alterations to the original painting. Some authors consider such varnishes to be suspect, suggesting that they might hide something [42]. Since the stylistic study suggested that some parts of the painting might be later additions, and to be sure that representative areas of the original paint (and later additions) were well documented, a large number of points [43] was initially measured with classic XRF, as indicated in Fig. 3.

Not all the results of individual measuring points are discussed separately here; only the main observations are summarised and discussed. The most significant finding is that high amounts of zinc and titanium are present irrespective of location and colour. In the stalk of the lilies (XRF4, XRF5), the red of the pomegranate (XRF14 and XRF24), the red of the grape leaf (XRF19) and the black background (XRF43) the amount of zinc is lower but is still measurable. Variations in the titanium signal are more difficult to follow, because the main titanium peaks ( $K\alpha$  at 4.509 keV and  $K\beta$  at 4.934 keV) coincide with barium peaks ( $L\alpha$  at 4.465 keV and  $L\beta$  at 4.842 keV), an element that is also frequently detected (but not at each measurement point). The variation in signal intensity of titanium seems to be similar to variations in the zinc signal intensity, implying that these elements occur together in the same matrix (paint). Zinc and titanium signals are remarkably high in the white of the lilies and in the white accents on the metal jug. The finding of titanium points to the presence of titanium white ( $TiO_2$ ), a pigment found

in artists' paints in two configurations: anatase and rutile. The distinction between these forms cannot be made with XRF, but MRS measurements confirmed that the titanium white is present in the anatase configuration. This pigment was manufactured on an industrial scale only from 1916 onwards, and used in painters' materials since 1921 [44]. The element zinc indicates more than likely zinc white ( $ZnO$ ), although zinc sulphide ( $ZnS$ ) cannot be ruled out. Zinc white is a synthetic inorganic pigment that was suggested as a pigment in 1783, but has only been used in oil painting since the 1830s, and more frequently since 1845 [43]. Zinc sulphide has been commercialized since 1852 [43]. The element barium was also detected in many measurement points (but not in XRF1, XRF2, XRF12, XRF20, XRF23, XRF30, XRF32, and XRF44), which is characteristic for the usage of barium sulphate ( $BaSO_4$ ), also of synthetic origin and marketed in the early 19th century [43]. When precipitated with  $ZnS$ , the pigment lithopone is obtained, commercialized since 1850, but only in mass production since 1874 [43]. All of these pigments are white, and can be used as pure white pigments, or mixed with other colours to make them lighter.

In the lilies, zinc white and titanium white are the most important white pigments. However, lead white [ $2PbCO_3 \cdot Pb(OH)_2$ ] was the main white pigment in 17th century painting. Lead is also detected at each measuring point, but in a surprisingly modest amount, as for example in the lemon in the basket (XRF15), leaf of the peach (XRF8), red of the lobster (XRF30, XRF31, XRF32) and white (XRF34) and yellowish-brown (XRF35) accents in the metal jug. Although still used in the 19th and 20th centuries, the simultaneous appearance of lead white and modern white pigments could indicate that the painting was heavily overpainted, as was suggested by the stylistic research.

In the red of the lobster (XRF30, XRF31, XRF31), selenium is detected in addition to cadmium (although only a very weak signal for cadmium was obtained). This indicates the use of cadmium red or orange. This pigment was not available in the 17th century and has only been commercialized since 1910 [45]. In other red parts, such as the pomegranate red (XRF24) and the red of a shrimp (XRF9), no cadmium red or orange is found. A second red pigment, vermilion, is indicated by the presence of mercury. Surprisingly, it is not found in red parts of the painting, but in the grey of the metal jug and in some of its yellow accents (XRF 33 to XRF37). Remarkable as well is the use of cadmium red or orange in the lobster, with vermilion employed for its reflection in the metal jug. The source of the vermilion is likely to be found in an underlying layer.

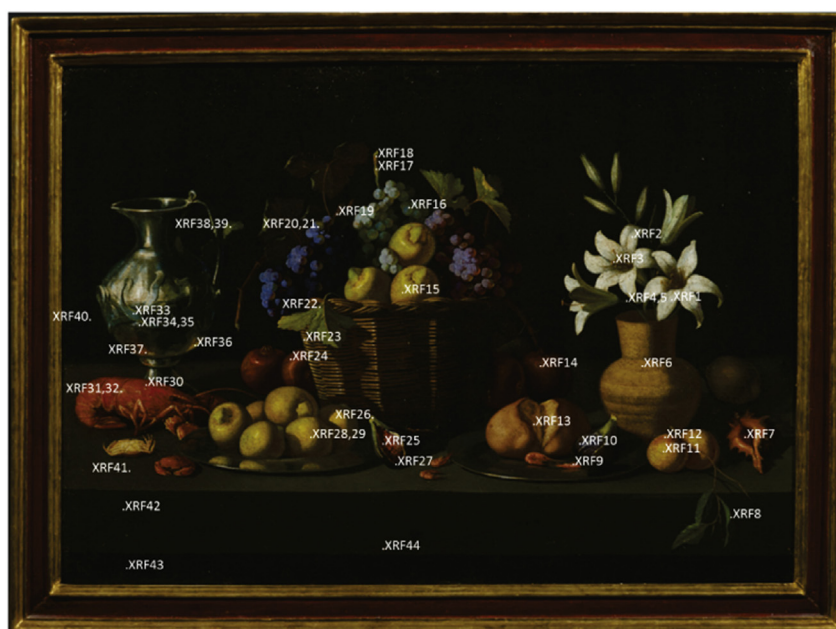


Fig. 3. Indication of the spots analysed by point XRF measurements.

In some parts of the painting, especially in the greyish table (XRF42, XRF43), cobalt, arsenic and nickel are found, which are characteristic of smalt, a cobalt-rich potassium glass. Used since the 15th century, smalt went slowly out of use after the discovery of Prussian blue in the early 18th century and cobalt blue at the end of the 18th century. It was hardly used in the 19th century [46]. In the blue of the grapes (XRF16 and XRF20) cobalt is also detected, but no arsenic and nickel, so it is likely that cobalt blue was used in this area. Again, the use of classic pigments next to modern alternatives is striking, and the only logical explanation seems to be the presence of hidden older paint layers.

Various colours in the painting did not produce XRF-signals. This is the case for the bright yellow of the lemons, (XRF15, XRF28, XRF29), the green leaf of the peach (XRF8) and the red of the pomegranates (XRF14 and XRF24). MRS analyses were performed directly on the painting, as the presence of synthetic organic pigments was suspected in these zones. As mentioned earlier, the thick layer of varnish caused measurement problems. The focus of the laser spot on the pigment grains is problematic and the varnish exhibits a strong fluorescence that masks the MRS signal. Data from strong Raman-scattering pigments could only be obtained in places where the varnish appeared to be thinner (tiny lacunae in the varnish). As mentioned earlier, anatase could be identified in different places. The main finding, however, was the presence of Pigment Green 8 (PG8) in the green leaf of the peach. PG8 belongs to the class of non-phthalocyanine metal complexes, discovered in 1885 but only commercially exploited since 1921 [47]. The structure of the pigment is essentially organic in nature, with an iron core. A slightly elevated iron signal is indeed detected with XRF, but most of the molecule is invisible to XRF. MRS analyses on the yellow of the lemons and the red of the pomegranates did not lead to useful Raman signals due to the strong fluorescence of the varnish.

Based on the results of the XRF and MRS analyses, it can be concluded that the still-life painting was not created in the 17th century; the presence of anatase all over the painting and PG8 in the leaf of the peach indicate that it cannot have been made before ca. 1921. Older pigments detected could be part of a hidden painting, implying that the canvas was re-used to make the still-life. Alternatively, the painting could have undergone a hyper-restoration, in which large parts of the original composition were overpainted or even removed during restoration [48,49]. An X-radiograph of the painting could have given more information, but this would have been expensive, and was difficult to justify in view of the doubts on the painting's authenticity. Therefore it was chosen to re-investigate the painting with MA-XRF.

Due to the dimensions of the painting, five individual MA-XRF maps were made. Elemental distribution maps for each element were then generated through manual stitching of the individual maps. As the painting was measured in its frame, the borders were not accessible. The total measuring time was around 10 h. Results of the MA-XRF analyses for the main elements detected are given as elemental distribution maps in Fig. 4.

These results confirm the occurrence of titanium and zinc in almost all points measured with classic XRF. Both elements are clearly present throughout the painting, except in the dark background. The distribution of zinc is analogous to that of titanium, as was also suggested by the point measurements; in the maps this is even more obvious as both images are practically identical, even in the grey intensity scale (although in some parts of the painting, zinc is absent when titanium is present, such as in the stork of the lilies, as was also observed by the point XRF analyses). Both elements must have been present in the same (commercial) paint, which was used in large parts of the painting and is not part of a later intervention.

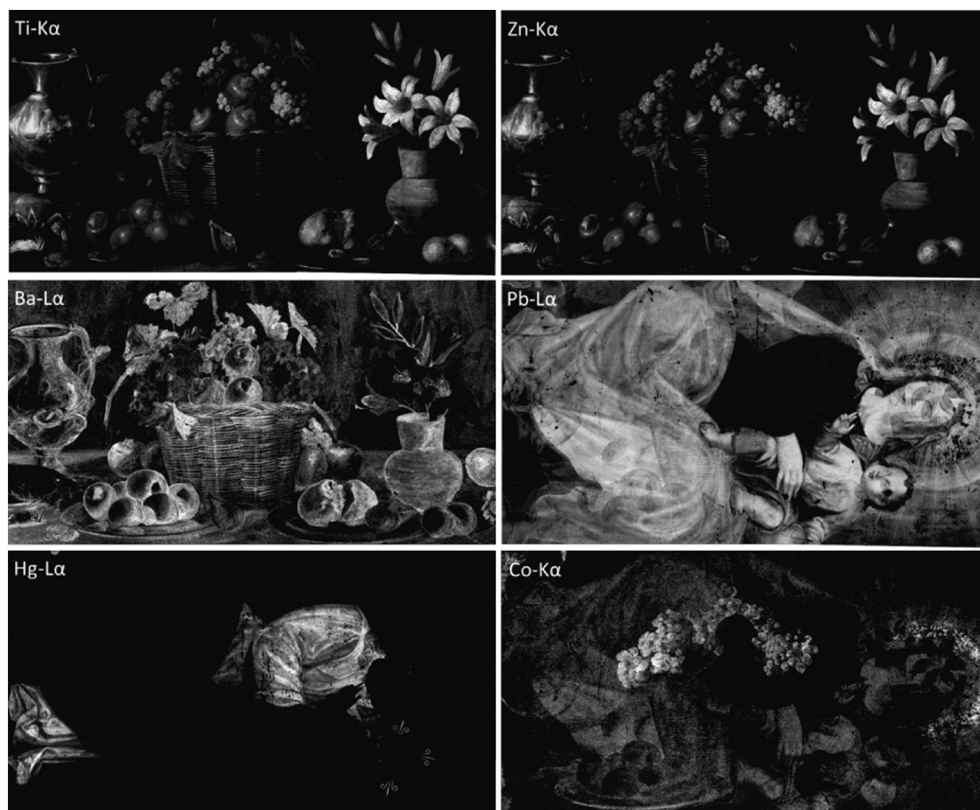


**Fig. 4.** Elemental distribution maps of a part of the Still-life painting obtained using macro X-ray fluorescence (MA-XRF) scanning. The distribution of the six main elements is shown: Ti, Zn, Ba, Pb, Hg and Co.

The distribution of barium (characteristic for barium sulphate) differs from the other two white pigments. It seems to be present everywhere, even in the dark background. In places where the zinc and titanium content is high, the barium signal is low and vice versa. This indicates that barium is present in an underlying layer, and that the barium signal is suppressed in places where zinc and titanium are present. Presumably it is present as pigment or cheap filler in a ground or isolation layer applied during execution of the still-life painting in order to mask what could be hidden below. The Ba-L $\alpha$  line is easily absorbed, implying that when it can be detected in an underlying layer, the upper layer must contain pigments that do not easily absorb X-rays. This suggests that the dark background is made up of a pigment composed of light elements such as carbon black. As barium can also be detected in relative high concentrations in certain parts of the painting, such as in the leaves above the fruit basket, it is likely also present on the surface mixed with other pigments as filling material or as a substrate for synthetic organic pigments.

The fourth white pigment identified - lead white - confirmed, as suspected, the presence of a hidden painting. The composition observed in the lead distribution map, represents a Virgin and Child. Paint losses in this first painting can be seen as black patches. These are quite limited, implying that the pictorial layer of the hidden painting is relatively undamaged. The lead distribution map proves that the still-life painting was made on a re-used canvas depicting another scene, ruling out the possibility of a hyper-restoration.

The elemental distribution maps of mercury and cobalt facilitate the interpretation and understanding of the point analyses. Vermilion has been used in the hidden painting for the dress of the Virgin (and in parts of the halo of the Child). As the metal jug has been partially painted over the dress, the presence of vermilion in the point analyses in the jug can easily be explained. MA-XRF distribution maps of selenium (not shown) confirm the usage of cadmium red (or orange) in the red lobster. The fact that no mercury was found despite the fact that the lobster is partially painted on the red dress of the Virgin was due to the local point measurements being carried out inadvertently in a paint loss in the red dress; hence only a signal of the modern cadmium rich paint was obtained. The reflection of the lobster in the jug is in fact painted with cadmium red (or orange), but this was not picked up in the point measurements due to the low concentration of cadmium; only a signal from the underlying vermilion in the red dress was measured. These observations also demonstrate that point measurements are not always representative for the whole paint surface.

The cobalt distribution map shows where cobalt rich pigments are present, but do not allow differentiation between smalt and cobalt blue. However, the images make it clear that cobalt is present both in the hidden painting as well as in the still-life, and easily localise zones with high cobalt intensity. As the images are the results of >3.7 million individual spectra, sum spectra of areas can be made. Two different spectra were obtained for the grapes and the Virgin's halo, although both are zones with relatively high cobalt signals. For the halo, arsenic and nickel were detected as well as cobalt, proving the presence of smalt, while in the blue grapes only cobalt was identified, pointing to cobalt blue.

As was the case for the point analyses, some colours cannot be identified by MA-XRF. These colours either contain elements too light to be detected (such as ultramarine) or are (synthetic) organic pigments. MA-XRF localises these zones, which could contain important information on the question of authenticity, especially when synthetic organic pigments are suspected [16,17]. For more precise and reliable pigment identification, MA-XRF scanning is best combined with (point measurement) methods providing molecular information such as MRS. However, as noted before, due to the thick varnish layer no further information could be obtained by MRS besides the detection of PG8.

It can be concluded that MA-XRF analyses of the painting allows a more straightforward interpretation of the XRF results in comparison with point XRF analyses. The MA-XRF elemental maps demonstrated

the presence of both modern and traditional pigments and proved without any doubt that the still-life was created after 1921, re-using an old canvas.

### 3.2. MA-XRF on the portrait of Jan Brant

The painting was first observed under UV light to localise possible retouching or overpaint (Fig. 2b). This revealed a varnish with a bluish fluorescence, as well as darker zones characteristic of later interventions. With point analyses these restored areas would have been avoided, as they would have provided false information. With MA-XRF, the painting surface can be completely analysed, although in this case only the central part was done (taking around 3 h). Unlike XRF, this technique allows the visualisation of later interventions, which are shown here in the elemental distribution maps of lead and calcium (Fig. 5). The dark patches in the lead distribution maps show losses in the paint. The actual damage to the paint is more limited than what the UV picture suggests; retouching was carried out on a wider area than the damage. The calcium distribution map is the inverse of the lead distribution map: the calcium signal intensity is more pronounced where losses occur, most likely because the calcium rich ground is exposed or because of the filling of the losses with a calcium rich material such as chalk or gypsum before retouching.

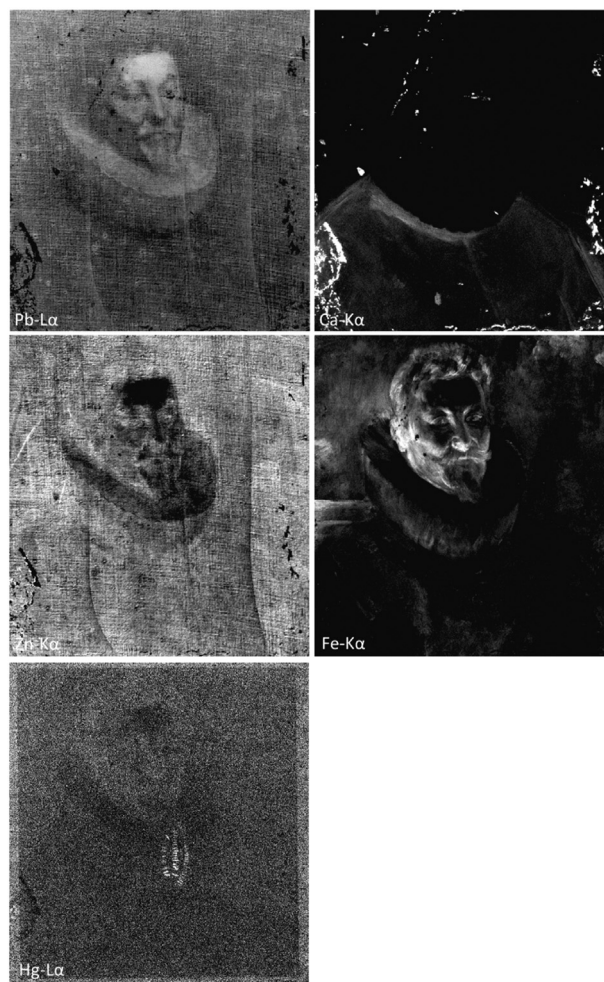
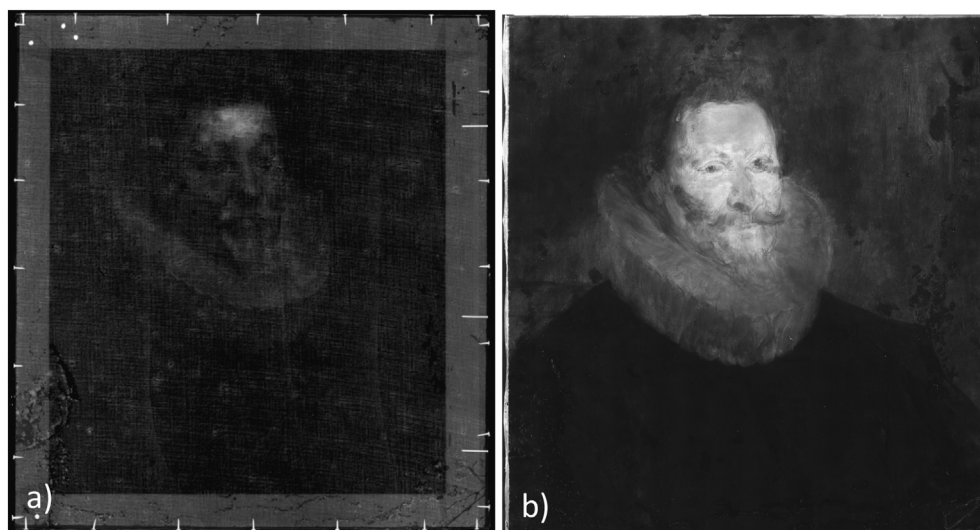


Fig. 5. Elemental distribution maps of a part of the Portrait of Jan Brant obtained using macro X-Ray fluorescence (MA-XRF) scanning. The distribution of the five main elements is shown: Pb, Ca, Zn, Fe and Hg.





**Fig. 6.** a) X-radiograph of the Portrait of Jan Brant. The results of the lead distribution map are quite similar to this image, although under the conditions used, the resolution of the X-radiograph is higher. Nonetheless, details of the face and ruff are more visible in the Pb distribution map. The hidden stamp cannot be seen. b) Infrared reflectogram of the painting, revealing underdrawings, but not the hidden stamp.

Lead is present throughout the painting and the canvas structure is visible in the lead distribution map, implying that the lead rich pigment, no doubt lead white, must be present in the ground or *imprimatura* layer. Lead is also present in the white areas of the paint, such as the ruff and flesh tones. The lead map is quite similar in appearance to the X-radiograph, although the latter is higher resolution (Fig. 6a) and reveals clearly a fine, even canvas weave. This already raises doubts as to the authenticity of the painting, as the weave is overly regular for a pre-industrial 17th century canvas. The resolution of the lead distribution map is lower, but could be improved by lowering the X-ray beam diameter and the distance between the measuring spots. As the main focus of the current study was the identification of the pigments, no attempt was made to gain a better image of the canvas structure using MA-XRF.

A third white pigment is detected, zinc white, as can be seen in the zinc distribution map. The damage to the paint is also visible in the zinc map, as is the structure of the canvas, implying that the zinc must be present in one of the preparatory layers and is close to or in contact with the canvas. Three vertical (dark) stripes are visible in the zinc map; these can also be observed in the lead distribution map as white patches, meaning that there is a higher lead concentration in these zones. It is likely that the lead rich layer has been applied with a palette knife or similar tool. Due to the higher lead density, the zinc signal is suppressed in these places, indicating that the zinc layer is actually present below the lead rich layer, and hence forms an integral part of the painting's layer structure.

The iron map reveals the distribution of iron rich pigments, likely earth pigments. Earth pigments have been popular since prehistory and are still frequently used, so do not provide additional information regarding a possible creation date. The iron concentration is especially high in the darker parts of the flesh tones, the hair and in the background. Near the right shoulder of Jan Brant there is a line that is not visible in the final image. In the original painting by Rubens in the *Alte Pinakothek* in Munich, the back of a chair can be seen at the same spot. In the present version, this chair was probably quickly sketched in using an iron rich painting medium, but was ultimately dropped.

The MA-XRF mercury distribution map revealed surprisingly precise information on the creation date of the painting: an original canvas stamp showing the name of the manufactory, stencilled on the canvas in vermilion based paint. The stamp is seen in reverse, implying it must be present on the back of the canvas. As the painting is relined, and there is no such stamp on the lining canvas, the stamp must be on

the back of the original support. Neither the X-radiograph nor the IRR image revealed it (Fig. 6a and b). To improve the stamp's readability, the area around it was reanalysed with a dwell time of 2 times 10 ms at higher resolution using a pixel size of 250  $\mu\text{m}$  and a 250  $\mu\text{m}$  X-ray beam diameter. The smaller X-ray beam diameter can be obtained by lowering the distance between the measuring head and the object. The M6 Jetstream features a poly-capillary lens, which generates a convergent X-ray beam to focus the X-ray tubes radiation. As an X-ray beam is typically broader below and above its focal plane, the X-ray beam size can be changed by changing the distance between the poly-capillary lens and the object, and hence by bringing the sample into focus (small X-ray beam diameter and small distance between object and poly-capillary lens) or out of focus (increase of the X-ray beam diameter and of the working distance between the object and the poly-capillary lens).

After mirroring the image and turning it clockwise 90°, the name of the manufacturer could be clearly read: "A. Schutzman" (Fig. 7). This canvas factory based in Munich was founded by August Schutzmann in 1844. The history of this firm has been traced by Beatrix Haaf [50]. In her publication she reproduces eight examples of the firm's canvas stamp, in chronological order. The full text of the stamp reads "*Malerleinwand Fabrik von A. Schutzman in MÜNCHEN*", translated as "Painting canvas manufactory of A. Schutzman in Munich". The stamp on the present painting corresponds well with a stamp in use in 1882 and in 1898. In Haaf's article, there is no precision as to the time periods in which the different stamps were used, but an earlier stamp with a slightly different appearance appears on a painting dated 1871/72. In 1902 another stamp design appears. This implies that the canvas used for the Portrait of Jan Brant can roughly be situated in between these two last dates, unless the Schutzmann firm used several stamps simultaneously. In any case, the painting cannot date to before the founding of the firm in 1844, which corresponds well with the MA-XRF pigment analyses results.

It is interesting to note that in 1836 the original version of the Portrait of Jan Brant entered the collections of the *Alte Pinakothek* in Munich, where it has been ever since. Therefore, at some point after 1836 the copyist could have set his easel up in the *Alte Pinakothek* museum and made his reduced version. It is worth noting that the IRR image reveals a sketchy, carbon-based underdrawing in a dry, non-friable medium, probably graphite (Fig. 8). The drawing is more detailed for the sitter's face, hair and ruff and both eyes have been moved up slightly during painting. The sketchiness of the drawing, together with the

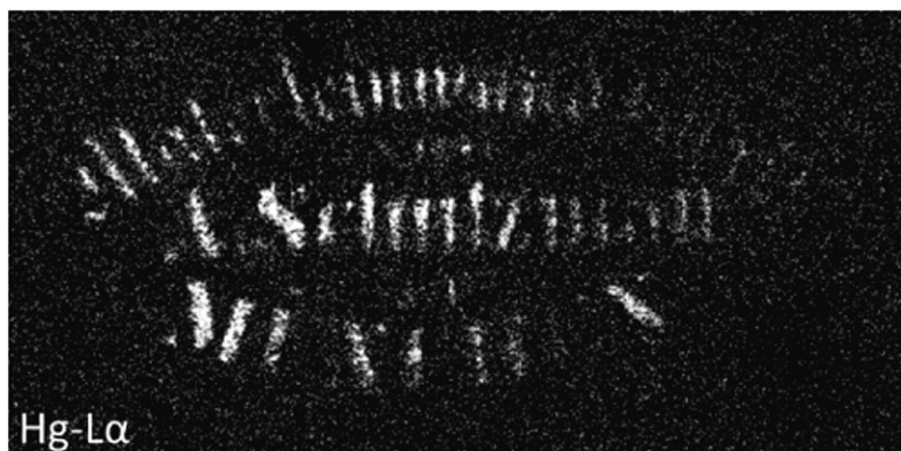


**Fig. 7.** Elemental distribution map of Hg of a detail of the Portrait of Jan Brant, showing the hidden stamp applied on the back of the original canvas. For ease of reading the stamp has been inverted and turned 90°.

shift of the eyes, suggests that the copy could have been made without a preliminary independent drawing, the artist working directly on his canvas after Rubens's original painting.

#### 4. Conclusion

MA-XRF scanning of two canvas paintings gives insights into the nature of their supports and painting materials and provides an answer to the question of their authenticity. This non-invasive method allowed the reconstruction of the artists' palettes, revealing pigments in both paintings that were not available in the time period that the paintings were assumed to have been made. In the case of the still life, initially attributed to Francisco de Zurbarán, point XRF-measurements had already suggested that the work could be a modern copy on an old canvas, although a hyper-restoration of the work could not be completely excluded. With MA-XRF, the chemical data, presented as elemental distribution map images, revealed a hidden painting underneath, simplifying the interpretation and explaining the results of the point analysis. Areas where (MA-)XRF results cannot explain the colours could point to the use of synthetic organic pigments, which are often of key importance for establishing execution dates. One such pigment, PG8, was indeed found in the painting.

In the Portrait of Jan Brant formerly attributed to Rubens's workshop or school, the presence of a hidden stamp of the canvas manufactory



**Fig. 8.** Detail of the infrared reflectogram of the Portrait of Jan Brant revealing sketchy underdrawing lines in the face; the arrows indicate the outline for the profile of the eyes, which are a little lower than their final painted position.

was discovered with MA-XRF. This stamp was not revealed in X-radiography or IRR. The identification of the manufactory gives an earliest possible creation date for the painting of 1844, and the design of the stamp suggests a likely execution period for the painting between 1871/72 and 1902, a few centuries later than originally supposed. MA-XRF also gave more information on the materials used, confirming the presence of zinc in or near the ground layer and therefore forming an integral part of the painting's layer structure. The lead distribution map produced comparable information to that obtained with X-radiography, although in lower resolution.

Although analyses with MA-XRF are rather slow, the operator needs only to be present to set-up the measurement. Once it is running, the instrument scans the painting (or parts of it) without any need for further intervention, making it a time-efficient process for the operator. This is not the case for XRF point analyses as the presence of an operator is required at all times. In a growing market, where there is a need for rapid and non-destructive methods of art authentication, MA-XRF could become a routine technique, complemented where necessary with molecular analyses such as micro-Raman spectroscopy.

#### Acknowledgement

We would like to express our gratitude to Catherine Fondaire for X-radiography, Sophie De Potter for infrared reflectography, and Stéphane Bazzo for the photography in normal and UV light. This research did not receive any specific grant from funding agencies in the public, commercial, or not-for-profit sectors.

#### References

- [1] P. Craddock, *Scientific Investigation of Copies, Fakes and Forgeries*, Butterworth-Heinemann, Oxford, 2007.
- [2] R. Adams, Pigments in the battle against forgery, *Focus. Pigment*. 2005 (2005) 1–3, [https://doi.org/10.1016/S0969-6210\(05\)70772-4](https://doi.org/10.1016/S0969-6210(05)70772-4).
- [3] M. Jones, P. Craddock, N. Barker (Eds.), *Fake? The Art of Deception*, First edition, University of California Press, 1990.
- [4] N. Chamey, *The Art of Forgery: The Minds, Motives and Methods of Master Forgers*, Phaidon Press Limited, London, 2015.
- [5] A. Amore, *The Art of the Con: The Most Notorious Fakes, Frauds, and Forgeries in the Art World*, 1st edition St. Martin's Press, 2015.
- [6] F.H. Kreuger, *A New Vermeer: Life and Work of Han Van Meegeren*, First edition Quantas Uitgevers, Delft, 2007.
- [7] J. Lopez, *The Man Who Made Vermeers: Unvarnishing the Legend of Master Forger Han van Meegeren*, First edition Houghton Mifflin Harcourt, Orlando, FL, 2008.
- [8] P. Coremans, *Van Meegeren's Faked Vermeers and De Hooghs: A Scientific Examination*, J.M. Meulenhoff, London/Amsterdam, 1949.
- [9] C. Irving, *FAKE! The Story of Elmyr de Hory, the Greatest Art Forger of Our Time*, McGraw-Hill, 1969.
- [10] L. Salisbury, A. Sujo, *Provenance: How a Con Man and a Forger Rewrote the History of Modern Art*, Penguin Books, First edition, 2010.
- [11] A. Birkenstock, *Beltracchi: The Art of Forgery*, 2015.



- [12] H. Beltracchi, W. Beltracchi, *Selbstporträt*, first edition Rowohlt Verlag GmbH, 2014.
- [13] D. Chappel, S. Hufnagel, The Beltracchi affair: a comment on the “most spectacular” German art forgery case in recent times, *J. Art Crime* (2012) 38–43 Spring 2012.
- [14] ABCnews item, In his own words: Pei Shen Qian talks art fraud, <http://abcnews.go.com/International/video/words-pei-shen-qian-talks-art-fraud-24622538>, Accessed date: 20 July 2017.
- [15] N. Khandekar, C. Mancusi-Ungaro, H. Cooper, C. Rosenberger, K. Eremin, K. Smith, J. Stenger, D. Kirby, A technical analysis of three paintings attributed to Jackson Pollock, *Stud. Conserv.* 55 (2010) 204–215.
- [16] S. Saverwyns, Russian avant-garde... or not? A micro-Raman spectroscopy study of six paintings attributed to Liubov Popova, *J. Raman Spectrosc.* 41 (2010) 1525–1532, <https://doi.org/10.1002/jrs.2654>.
- [17] S. Saverwyns, W. Fremout, Genuine or fake: a micro-raman spectroscopy study of an abstract painting attributed to Vasily Kandinsky, *Proc. Art11 CD, AIPnD, Florence*, 2011.
- [18] T.D. Chaplin, R.J.H. Clark, Identification by Raman microscopy of anachronistic pigments on a purported Chagall nude: conservation consequences, *Appl. Phys. A Mater. Sci. Process.* 122 (2016), 144, <https://doi.org/10.1007/s00339-016-9644-3>.
- [19] N. Eastaugh, Authenticity and the Scientific Method, 1, *InCoRM*, 2009 3–12.
- [20] N. Charney, Forging for fame: case studies of Ken Perenyi and Wolfgang Beltracchi, *J. Art Crime* (2016) 87–91 Spring 2016.
- [21] J. Lang, A. Middleton (Eds.), *Radiography of Cultural Material*, 2nd edition Routledge, Amsterdam, 2005.
- [22] The Closer to Van Eyck website gives more information on IRR, including many examples, <http://closerovaneyck.kikirpa.be>, Accessed date: 22 September 2017.
- [23] J. Ragai, *The Scientist and the Forger*, Imperial College Press, first edition, 2015 <http://www.worldscientific.com/worldscibooks/10.1142/p1019>, Accessed date: 20 July 2017.
- [24] F. Schulte, K.-W. Brzezinka, K. Lutzenberger, H. Stege, U. Panne, Raman spectroscopy of synthetic organic pigments used in 20th century works of art, *J. Raman Spectrosc.* 39 (2008) 1455–1463, <https://doi.org/10.1002/jrs.2021>.
- [25] N.C. Scherrer, S. Zumbuehl, F. Delavy, A. Fritsch, R. Kuehnen, Synthetic organic pigments of the 20th and 21st century relevant to artist's paints: Raman spectra reference collection, *Spectrochim. Acta A Mol. Biomol. Spectrosc.* 73 (2009) 505–524, <https://doi.org/10.1016/j.saa.2008.11.029>.
- [26] W. Fremout, S. Saverwyns, Identification of synthetic organic pigments: the role of a comprehensive digital Raman spectral library, *J. Raman Spectrosc.* 43 (2012) 1536–1544, <https://doi.org/10.1002/jrs.4054>.
- [27] K. Lutzenberger, *Künstlerfarben im Wandel: Synthetische organische Pigmente des 20. Jahrhunderts und Möglichkeiten ihrer zerstörungsarmen, analytischen Identifizierung*, Utz, Herbert, München, 2009.
- [28] J. Russell, *A Study of the Materials and Techniques of Francis Bacon (1909–1992)* PhD Northumbria University, 2010.
- [29] F. Rosi, C. Grazia, R. Fontana, F. Gabrieli, L. Pensabene Buemi, E. Pampaloni, A. Romani, C. Stringari, C. Miliani, Disclosing Jackson Pollock's palette in *Alchemy (1947)* by non-invasive spectroscopies, *Herit. Sci.* 4 (2016), 18, <https://doi.org/10.1186/s40494-016-0089-y>.
- [30] A. Duran, M.L. Franquelo, M.A. Centeno, T. Espejo, J.L. Perez-Rodriguez, Forgery detection on an Arabic illuminated manuscript by micro-Raman and X-ray fluorescence spectroscopy, *J. Raman Spectrosc.* 42 (2011) 48–55, <https://doi.org/10.1002/jrs.2644>.
- [31] M. Alfeld, K. Janssens, J. Dik, W. de Nolf, G. van der Snickt, Optimization of mobile scanning macro-XRF systems for the in situ investigation of historical paintings, *J. Anal. At. Spectrom.* 26 (2011) 899–909, <https://doi.org/10.1039/C0JA00257G>.
- [32] M. Alfeld, J.V. Pedroso, M. van E. Hommes, G.V. der Snickt, G. Tauber, J. Blaas, M. Haschke, K. Erler, J. Dik, K. Janssens, A mobile instrument for in situ scanning macro-XRF investigation of historical paintings, *J. Anal. At. Spectrom.* 28 (2013) 760–767, <https://doi.org/10.1039/C3JA30341A>.
- [33] M. Alfeld, G.V. der Snickt, F. Vanmeert, K. Janssens, J. Dik, K. Appel, L. van der Loeff, M. Chavannes, T. Meedendorp, E. Hendriks, Scanning XRF investigation of a flower still life and its underlying composition from the collection of the Kröller–Müller museum, *Appl. Phys. A Mater. Sci. Process.* 111 (2013) 165–175, <https://doi.org/10.1007/s00339-012-7526-x>.
- [34] R. Alberti, T. Frizzi, L. Bombelli, M. Gironda, N. Aresi, F. Rosi, C. Miliani, G. Tranquilli, F. Talarico, L. Cartechini, CRONO: a fast and reconfigurable macro X-ray fluorescence scanner for in-situ investigations of polychrome surfaces, *X-Ray Spectrom.* (2017) <https://doi.org/10.1002/xrs.2741> (n/a-n/a).
- [35] F.P. Romano, C. Caliri, P. Nicotra, S.D. Martino, L. Pappalardo, F. Rizzo, H.C. Santos, Real-time elemental imaging of large dimension paintings with a novel mobile macro X-ray fluorescence (MA-XRF) scanning technique, *J. Anal. At. Spectrom.* 32 (2017) 773–781, <https://doi.org/10.1039/C6JA00439C>.
- [36] M. Alfeld, D.P. Siddons, K. Janssens, J. Dik, A. Woll, R. Kirkham, E. van de Wetering, Visualizing the 17th century underpainting in portrait of an old man by Rembrandt van Rijn using synchrotron-based scanning macro-XRF, *Appl. Phys. A Mater. Sci. Process.* 111 (2013) 157–164, <https://doi.org/10.1007/s00339-012-7490-5>.
- [37] L.S. Van der Loeff, M. Alfeld, T. Meedendorp, J. Dik, E. Hendriks, G. Van der Snickt, K. Janssens, M. Chavannes, Rehabilitation of a flower still life in the Kröller–Müller Museum and a lost Antwerp painting by Van Gogh, in: L. Van Tilborgh (Ed.), *Van Gogh New Find*, WBOOKS, Zwolle 2012, pp. 33–53.
- [38] P.P. Rubens, Portrait of Jan Brant, 17th century, [https://commons.wikimedia.org/wiki/Category:Paintings\\_by\\_Peter\\_Paul\\_Rubens\\_in\\_the\\_Alte\\_Pinakothek#/media/File:Peter\\_Paul\\_Rubens\\_\(1577-1640\)\\_Jan\\_Brant\\_\(vader\\_van\\_Isabella\)\\_Alte\\_Pinakothek\\_25-01-2017\\_16-21-00.jpg](https://commons.wikimedia.org/wiki/Category:Paintings_by_Peter_Paul_Rubens_in_the_Alte_Pinakothek#/media/File:Peter_Paul_Rubens_(1577-1640)_Jan_Brant_(vader_van_Isabella)_Alte_Pinakothek_25-01-2017_16-21-00.jpg), Accessed date: 20 July 2017.
- [39] H. Bronk, S. Röhrs, A. Bjeoumikhov, N. Langhoff, J. Schmalz, R. Wedell, H.E. Gorny, A. Herold, U. Waldschläger, ArtTAX—a new mobile spectrometer for energy-dispersive micro X-ray fluorescence spectrometry on art and archaeological objects, *Fresenius J. Anal. Chem.* 371 (2001) 307–316.
- [40] D.S. Bright, D.E. Newbury, Maximum pixel spectrum: a new tool for detecting and recovering rare, unanticipated features from spectrum image data cubes, *J. Microsc.* 216 (2004) 186–193, <https://doi.org/10.1111/j.0022-2720.2004.01412.x>.
- [41] W. Fremout, S. Saverwyns, F. Peters, D. Deneffe, Non-destructive micro-Raman and X-ray fluorescence spectroscopy on pre-Eyckian works of art-verification with the results obtained by destructive methods, *J. Raman Spectrosc.* 37 (2006) 1035–1045, <https://doi.org/10.1002/jrs.1610>.
- [42] R.H. Marijnissen, *Paintings Genuine, Fraud, Fake: Modern Methods of Examining Paintings*, first edition Elsevier Librico, Belgium, Brussels, 1985.
- [43] N. Eastaugh, V. Walsh, T. Chaplin, R. Siddall, *Pigment Compendium: A Dictionary of Historical Pigments*, Elsevier Butterworth-Heinemann, Amsterdam; Boston, 2004.
- [44] M. Laver, Titanium Dioxide Whites, in: E. West FitzHugh (Ed.), *Artists' Pigments: A Handbook of Their History and Characteristics*, 3, National Gallery of Art-Washington/Oxford University Press 1997, pp. 295–355.
- [45] I. Fiedler, M. Bayard, Cadmium yellows, oranges and reds, in: I. Feller, L. Robert (Eds.), *Artists' Pigments. A Handbook of Their History and Characteristics*, 1, National Gallery of Art, Washington & Cambridge University Press 1986, pp. 65–108.
- [46] B. Mühlethaler, J. Thissen, Smalt, in: R. Ashok (Ed.), *Artists' Pigments. A Handbook of Their History and Characterisation*, Archetype Publications, London 1993, pp. 113–130.
- [47] W. Herbst, K. Hunger, *Industrial Organic Pigments: Production, Properties, Applications*, 2nd edition Wiley-VCH, Weinheim, 2004.
- [48] H. Verougstraete, R. Van Schoute, T.-H. Borchert, E. Bruyns, J. Couvert, R. Pieters, J.-L. Pypaert, Fake or not fake: het verhaal van de restauratie van de Vlaamse Primitieven, Ludion, Gent, 2004.
- [49] D. Vanwijnsberghe, C. Bourguignon, J. Debergh, C. Fondaire, P. Fraiture, S. Laemers, J. Lust, D. Martens, L. Mortiaux, P. Philipot, J.-L. Pypaert, J. Sanyova, S. Saverwyns, *Autour de la Madeleine Renders: un aspect de l'histoire des collections, de la restauration et de la contrefaçon en Belgique dans la première moitié du XXe siècle*, Koninklijk Instituut voor het Kunstpatrimonium, Brussel, 2008.
- [50] B. Haaf, Industriell vorgründerte Malleinen: Beiträge zur Entwicklungs- Handels und Material Geschichte, *Z. Für Kunsttechnol. Konserv.* 2 (1987) 7–71.